

# Rapid and quantitative DNA analysis of genetic mutations for polycystic kidney disease (PKD) using magnetic/luminescent nanoparticles

Ahjeong Son · Amy Dhirapong · Dosi K. Dosev ·  
Ian M. Kennedy · Robert H. Weiss ·  
Krassimira R. Hristova

Received: 30 October 2007 / Revised: 11 January 2008 / Accepted: 17 January 2008 / Published online: 7 February 2008  
© Springer-Verlag 2008

**Abstract** Rapid and accurate detection of genetic mutations based on nanotechnology would provide substantial advances in detection of polycystic kidney disease (PKD), a disease whose current methods of detection are cumbersome due to the large size and duplication of the mutated gene. In this study, a nanotechnology-based DNA assay was developed for detection of SNPs (single nucleotide polymorphisms) in a feline autosomal dominant PKD (ADPKD) model which can readily be adapted to diagnosis of human ADPKD type 1. Europium and terbium phosphors were doped into gadolinium crystal hosts with a magnetic core, providing stable luminescence and the possibility of magnetic manipulations in a solution-based assay. A hybridization-in-solution DNA assay was optimized for feline PKD gene SNP detection using genomic

DNA extracted from feline kidney tissue and blood. This assay showed a substantial differentiation between PKD and control specimens. The nanotechnology-based DNA assay is attractive from the viewpoint of rapid availability, simple methodology, and cost reduction for clinical use to detect mutations involved in human ADPKD and other genetic diseases.

**Keywords** Polycystic kidney disease (PKD) · DNA · Single nucleotide polymorphisms (SNPs) · Nanoparticles · Hybridization-in-solution · Lanthanide oxide

## Introduction

The presence and precise location of genetic mutations determine prognosis and response to currently used or investigative drugs. The rapid and inexpensive determination of these mutations has the potential to revolutionize the diagnosis and treatment of diseases ranging from cancer to hereditary diseases. In addition, identification of mutations in family members of affected patients will allow proper planning and treatment prior to clinical onset of the disease.

Nanoscale technology offers numerous advantages for detection of genetic mutations, such as very large surface areas for the immobilization of bio-recognition elements, easy manipulation/diffusion within samples, and size compatibility with DNA as a target. Recent progress in nanoparticle applications allowed detection of SNPs mutations in the genes related to cancer [1], genetic disease [2], and nitrification [3] by gold nanoparticles [2, 4–6], quantum dots nanocrystals [1], and silica nanoparticles [3]. However, the listed efforts were mostly limited to synthetic ssDNA target (proof-of-concept study) [1, 3–5],

---

A. Son · K. R. Hristova (✉)  
Department of Land, Air, and Water Resources,  
University of California, Davis,  
1 Shields Avenue,  
Davis, CA 95616, USA  
e-mail: krhristova@ucdavis.edu

D. K. Dosev · I. M. Kennedy  
Department of Mechanical and Aeronautical Engineering,  
University of California, Davis,  
1 Shields Avenue,  
Davis, CA 95616, USA

A. Dhirapong · R. H. Weiss  
Division of Nephrology, Department of Internal Medicine,  
University of California, Davis,  
1 Shields Avenue,  
Davis, CA 95616, USA

R. H. Weiss  
VA Northern California Health Care System,  
Sacramento, CA 95655, USA

target-amplification typically with PCR [6], or/and requirement of specific instruments (i.e. microarrays and scanners) [2, 6]. Those shortcomings ultimately limit the current utility of nanotechnology solutions in applications such as clinical diagnosis.

Autosomal dominant polycystic kidney disease (ADPKD) is one of the most common genetic disorders in humans [7, 8] and is the most common inherited kidney disease. ADPKD is characterized by enlarged polycystic organs and is progressive, leading to end-stage renal disease in late middle age with complications that are associated with hemodialysis [8, 9]. ADPKD results from mutations in two genes, PKD1 (responsible for 85% of ADPKD cases) and PKD2 [9–11]. Molecular diagnosis of PKD generally involves (RT)-PCR/sequencing-based methods [12, 13] which are cumbersome and time consuming, and often classified as costly “send-out” tests. As an alternative, detection of DNA mutations based on rapid and sensitive nanotechnology could be regularly utilized in the clinic and thus result in much earlier (even pre-natal) diagnosis of PKD.

As shown previously [14],  $\text{Fe}_3\text{O}_4/\text{Eu}:\text{Gd}_2\text{O}_3$  core-shell nanoparticles were designed to achieve multi-functional advantages. The magnetic property of nanoparticles (NPs) enables efficient separation of NP-DNA hybrids from solution, which expedites the assay. The stable and long-lasting luminescence from lanthanide phosphors serves as an internal calibration for organic dye labels ( $F_{\text{dye}}/F_{\text{NPs}}$ ) [15, 16]. Furthermore, the use of spray pyrolysis in NP synthesis [15, 17] enables reduction of the production cost, which often limits the wide applicability of other NP-based technologies.

In this study, we have developed a rapid, accurate, and inexpensive NPs-DNA based assay to detect PKD SNP mutations in hybridization-in-solution platform. A feline PKD model was selected due to the marked similarity of feline PKD to human PKD [18], greater than most other currently available animal models. Genomic DNA isolated from feline kidney tissue and blood was used as a target of direct hybridization. The optimized NPs-DNA-based assay is a major advance in SNPs detection, resulting in the potential for more general and widespread use of this ADPKD diagnostic test in the clinic.

## Materials and methods

### Materials and instrumentation

Linear DNA oligoprobes were designed based on the sequences of feline PKD exon29 and 38 genes (Genbank accession for exon29: AY612847, exon38: AY612849) [19] and commercially synthesized (IDT, Coralville, IA, USA). NeutrAvidin (NA) and bovine serum albumin (BSA) were

purchased from Pierce (Rockford, IL, USA) and Sigma (St Louis, MO, USA), respectively. Takara EX *Taq* PCR enzyme and buffers were obtained from Takara Bio (Madison, WI, USA).

A Spectramax M2 microplate reader (Molecular Devices, Sunnyvale, CA, USA) and black 96-well plates (Nunc, Roskilde, Denmark) were used for fluorescence detection. A magnetic separation of NP-DNA hybrids was performed with MPC-S magnet (Dynal-Invitrogen, Carlsbad, CA, USA). A hybridization incubator (Hybridizer HB1-D, Techne, Burlington, NJ, USA) was used to provide a constant temperature (37 °C) and gentle mixing for the DNA hybridization and/or protein encapsulation of NPs. A sonic dismembrator (Fisher Scientific, Pittsburgh, PA, USA) was used to denature genomic DNA by ultrasonication. A Techne (TC-412, Burlington, NJ, USA) PCR machine was used for PCR amplification of feline genomic DNA. DNA (at  $\lambda=260$  nm) and protein (at  $\lambda=595$  nm) concentrations were measured by means of a UVmini 1240 UV-visible spectrophotometer (Shimadzu, Kyoto, Japan).

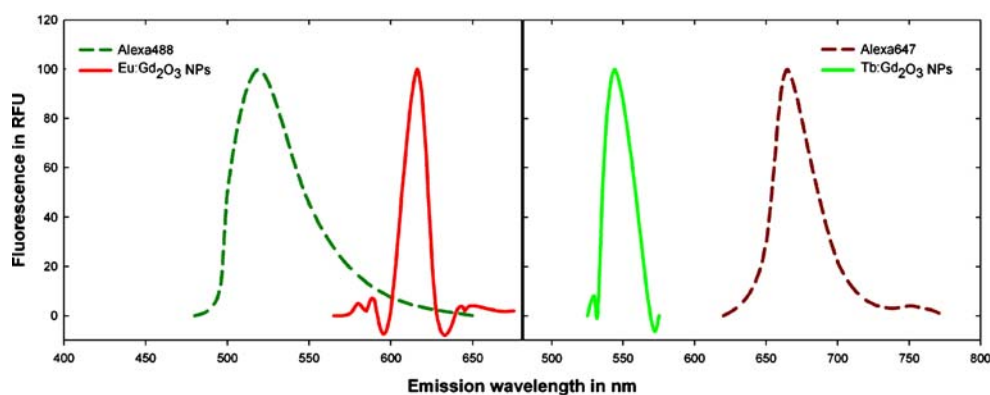
### Surface functionalization of NPs

The  $\text{Fe}_3\text{O}_4/\text{Eu}:\text{Gd}_2\text{O}_3$  and  $\text{Fe}_3\text{O}_4/\text{Tb}:\text{Gd}_2\text{O}_3$  core-shell nanoparticles (NPs) used in this work were synthesized by the spray pyrolysis and precipitation processes [15, 19]. NPs were functionalized by passive adsorption of neutravidin (NA). In the current study, NA was directly quantified instead of using indirect quantification based on the fluorescence of Alexa555-conjugated streptavidin [14]. To determine the optimum amount, NA was quantified before and after incubation with NPs using the Bradford protein assay [20] with dual standards (BSA and NA). The absorbance was measured at 595 nm using a standard curve constructed after analysis of known concentrations of BSA and NA. Three types of phosphate-based buffer, PB (phosphate buffer, 25 mmol L<sup>-1</sup>, pH 7.5), PBS (phosphate-buffered saline, 10 mmol L<sup>-1</sup>, pH 7.4, 0.8% saline), and PBST (PBS-Tween, 10 mmol L<sup>-1</sup>, pH 7.4, 0.05% Tween 20), were tested for choice of the optimal buffer for NPs-functionalization.

### Hybridization in solution using NP-DNA probes

In order to examine two mutational points in the feline model, two different lanthanide-doped (europium and terbium) nanoparticles were paired with reporter organic dyes (Alexa488 and Alexa647, respectively) for SNPs detection. The emission spectra of lanthanide NPs and reporter dyes are shown in Fig. 1. NA-encapsulated NPs were mixed with 1000  $\mu\text{L}$  DIG easy Hyb buffer (Roche, Basel, Switzerland) and biotinylated probe DNA. Two allele-specific probes were designed to cover the SNP sites

**Fig. 1** Fluorescence emission spectra of Eu:Gd<sub>2</sub>O<sub>3</sub> NPs ( $\lambda_{\text{ex}}=260$  nm), Alexa488 organic dye ( $\lambda_{\text{ex}}=495$  nm), Tb:Gd<sub>2</sub>O<sub>3</sub> NPs ( $\lambda_{\text{ex}}=260$  nm), and Alexa647 ( $\lambda_{\text{ex}}=650$  nm). NPs, nanoparticles



of exon29 and 38. The hybridization mixture was incubated for 2 h at 37 °C with gentle rotation. Following washing three times with phosphate buffer (25 mmol L<sup>-1</sup>, pH 7.5), both Eu:Gd<sub>2</sub>O<sub>3</sub>/Fe<sub>3</sub>O<sub>4</sub> and Tb:Gd<sub>2</sub>O<sub>3</sub>/Fe<sub>3</sub>O<sub>4</sub> NP-probe DNA conjugates were hybridized for 8 h at 37 °C with different amounts of target DNAs, labeled with Alexa488 and Alexa647. The fluorescence of Alexa488 ( $\lambda_{\text{ex}}=495$  nm,  $\lambda_{\text{em}}=519$  nm), Alexa647 ( $\lambda_{\text{ex}}=650$  nm,  $\lambda_{\text{em}}=665$  nm), europium ( $\lambda_{\text{ex}}=260$  nm,  $\lambda_{\text{em}}=616$  nm), and terbium ( $\lambda_{\text{ex}}=260$  nm,  $\lambda_{\text{em}}=544$  nm) were measured in a microplate reader at 26 °C.

#### gDNA extraction, denaturation, and PCR amplification

Feline kidney tissue and blood samples (Persian cats of ADPKD positive/negative) were obtained from Dr Leslie Lyons' laboratory in the School of Veterinary Medicine at UC Davis. Prior to gDNA extraction, kidney tissue was incubated with RNase A, in order to remove RNA which exists at high level in transcriptionally active kidney tissue. White blood cells (WBC) were separated from whole blood by centrifugation (5000 rpm, 15 min) at room temperature. Genomic DNA was extracted from the WBC-enriched fraction by using the QIAamp DNA mini kit (Qiagen, Valencia, CA, USA) and subsequently denatured by incubation at 95 °C for 5 min and following ultrasonication for 30 s. Exon29 polymorphism (C → A transversion) was selected for the following experiments due to the significance of the exon29 mutation in causing a stop codon that results in production of an abnormal, truncated protein, while exon38 polymorphism (C → T) links to only amino acid change without protein alteration [18]. PCR (polymerase chain reaction) was implemented to verify that exon29 SNP existed in the extracted gDNA and to permit use of the amplified PKD gene (~550 bp) as a target during the initial assay optimization and detection with DNA signaling probe. Touchdown PCR (59 °C → 50 °C, decreasing 0.5° per cycle) was performed using a primer set targeting feline PKD gene exon29 (FW 5' CAGGTAGACGGGATAGACGA 3', RV 5' TTCTTCCTGGTCAACAGCTG 3') [18]. PCR

amplicons were purified using the Qiagen PCR purification kit and their size was confirmed by horizontal 1.5% agarose gel electrophoresis.

#### PKD SNPs detection in gDNA from feline kidney tissue and blood

Aiming to pinpoint the optimum conditions for PKD SNPs detection in feline gDNA, hybridization buffer composition and gDNA denaturation were optimized. Concentrations varied from 30 to 250 mmol L<sup>-1</sup> NaCl and from 0 to 70% formamide. Following to hybridization of gDNA without PCR amplification using NP-probe DNA and signaling probe DNA labeled with Alexa488, three rounds of washing were performed by using 10 mmol L<sup>-1</sup> PB, 300 mmol L<sup>-1</sup> NaCl buffer in a magnet-separation platform.

## Results and discussion

### Magnetic/luminescent nanoparticles

The current NPs-based approach for SNPs detection of the PKD gene makes use of our experience with Fe<sub>3</sub>O<sub>4</sub>/Eu:Gd<sub>2</sub>O<sub>3</sub> core-shell nanoparticles in quantitative detection of bacterial 16S rRNA gene [14] and quantitative immunoassays [15, 16]. Detailed characterization of our lanthanide NPs has been described elsewhere [15, 21]. The multifunctional magnetic/luminescent NPs used here have diameters of about 200–400 nm, which is reasonably compatible with the size of DNA molecules and permits an efficient interaction between nanoparticles and DNA probes. The magnetic property of NPs allows separation of the DNA–NP complexes from solution. The lanthanide NPs are inherently photostable with a long fluorescence lifetime (~1 ms); their signal provides a normalization signal for the fluorescence from the organic dye labels ( $F_{\text{dye}}/F_{\text{NPs}}$ ). Figure 1 shows the emission spectra of both NPs (Fe<sub>3</sub>O<sub>4</sub>/Eu:Gd<sub>2</sub>O<sub>3</sub>, Fe<sub>3</sub>O<sub>4</sub>/Tb:Gd<sub>2</sub>O<sub>3</sub>) and Alexa dyes used in this study. We have used the optimal excitation wavelength to

excite each Alexa dye and NPs individually. Europium and terbium have significantly narrower emission lines (at  $\lambda=616$  nm and  $\lambda=544$  nm) than organic dyes, which is a promising characteristic that may be exploited for multiplexed analyses.

The NPs were biofunctionalized with neutravidin (NA); DNA probes were attached as described by Son et al. [14]. The optimum concentrations of the coating reagent (NA/mg NPs) and buffer of choice were determined by direct quantification of NA (Fig. 2). The absorbance of NA in solution was measured before and after incubation with NPs. A varying amount of NA (10, 20, 50, 100, 200  $\mu\text{g}$ ) per 1 mg NPs was added to series of incubation reactions in PB, PBS, and PBST buffers. The higher concentrations of adsorbed NA were 4.51  $\mu\text{g}$  (50  $\mu\text{g}$  NA was added) and 4.43  $\mu\text{g}$  (100  $\mu\text{g}$  NA) (Table 1). Even though the actual adsorbed amount of NA on the NPs' surface was similar when concentrations of 50 or 100  $\mu\text{g}$  NA/mg NPs were tested, the optimum NA coating amount was selected to be 50  $\mu\text{g}$  per 1 mg NPs, due to the higher efficiency of adsorption of 50  $\mu\text{g}$  NA (~50%) compared with 100  $\mu\text{g}$  NA (~30%). Based on the amount of NA coated on NPs' surface, PB was selected to be the optimum buffer among those tested: PB, PBS, and PBST. The concentration of adsorbed NA ( $\mu\text{g}$ ) was also converted to pmoles based on the molecular weight of NA (60,000) (Table 1). For subsequent hybridization experiments, the amount of biotinylated DNA probe (20 pmol) was determined on the basis of the amount of NA adsorbed on the NPs surface (7.5 pmol).

**Table 1** Surface functionalization of NPs

Added NA ( $\mu\text{g}$ NA/mg NPs)	NA adsorbed on NPs	
	( $\mu\text{g}$ NA/mg NPs)	(pmoles NA/mg NPs)
10	0.266	0.44
20	0.236	0.39
<b>50</b>	<b>4.514</b>	<b>7.52</b>
100	4.426	7.37
200	2.390	4.00

The amount of NA adsorbed on the NPs' surface was measured by the Bradford protein quantification assay [20]. The adsorbed NA was calculated based on the measurement of free NA in solution before and after incubation. The optimum NA amount (in bold) was selected to be 50  $\mu\text{g}/\text{mg}$  NPs in PB buffer. PB, phosphate buffer; NA, neutravidin

### Hybridization of NP-probes and ssDNA targets

Two naturally occurring PKD point mutations in the feline model were examined to confirm that this newly developed nanotechnology can distinguish single nucleotide polymorphisms, and to ensure that SNPs detection is feasible for more than one genomic location. A hybridization-in-solution assay (Fig. 2) using NP-probes and synthetic ssDNA (single stranded DNA) targets was performed, and the DNA-hybrids were separated out of the hybridization solution by a magnet [14]. DNA sequences were discriminated by a difference in fluorescence signal of PKD negative (cytosine) and positive (adenine) in exon29 (Fig. 2a) and negative (cytosine) and positive (thymine) in

**Fig. 2** PKD SNPs detection assay using synthetic ssDNA probes on a hybridization-in-solution platform for (a) exon29 and (b) exon38 polymorphism. Eu:Gd<sub>2</sub>O<sub>3</sub>/Fe<sub>3</sub>O<sub>4</sub> - Alexa488 and Tb:Gd<sub>2</sub>O<sub>3</sub>/Fe<sub>3</sub>O<sub>4</sub> - Alexa647 labels were used for exon29 and exon38 SNPs detection, respectively. The 1 bp difference in the nucleotide sequences of PKD+ and PKD- synthetic DNA are shown. The signal and error bars represent average and standard deviations based on triplicate reactions. PKD, polycystic kidney disease; SNPs, single nucleotide polymorphisms; RFU, relative fluorescence units

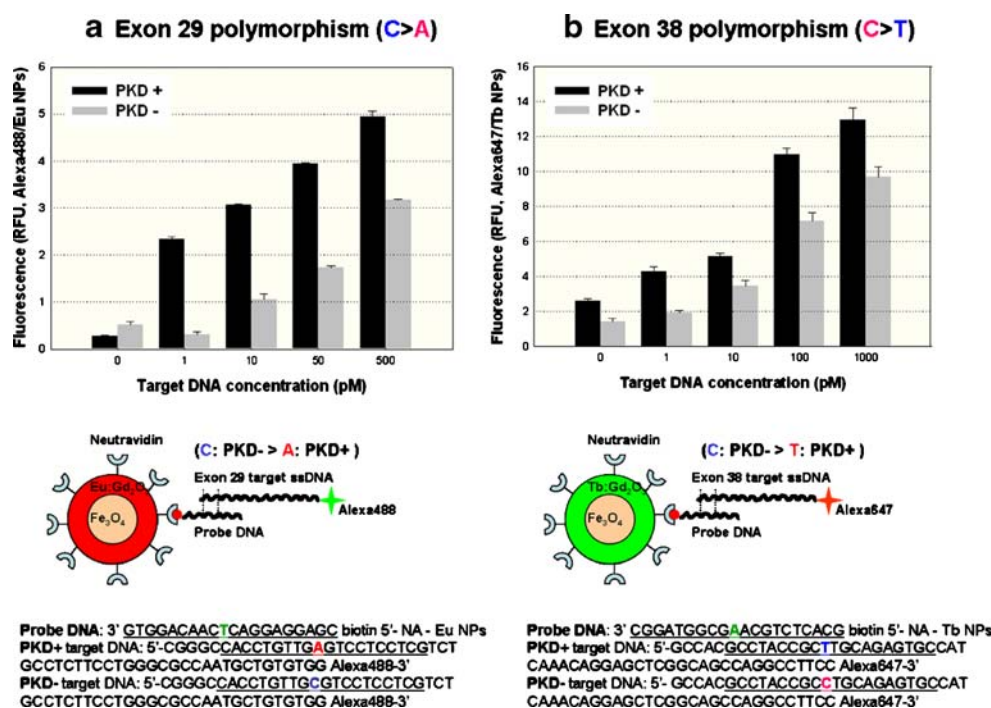
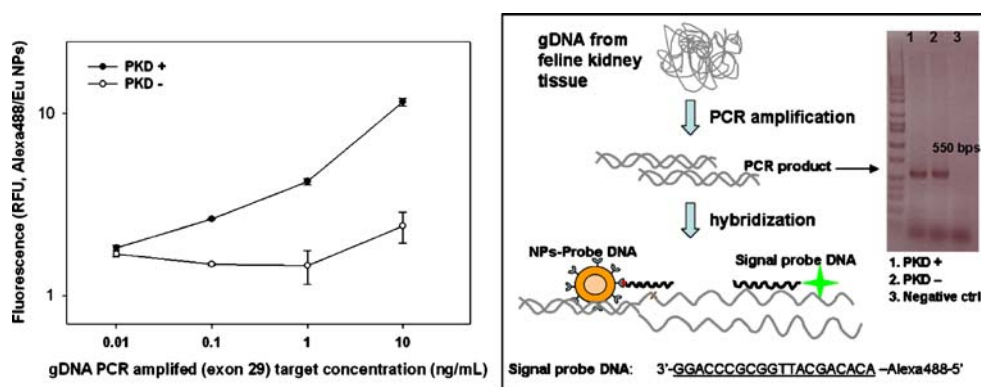


**Fig. 3** PKD SNPs detection assay using PCR-amplified genomic DNA (feline exon29, 550 bp product). A signaling probe was used to provide fluorescence by Alexa488 labeling. The signal and error bars represent average and standard deviations based on triplicate reactions. The band on the agarose gel photo indicates 550 bp PCR product amplified from feline gDNA



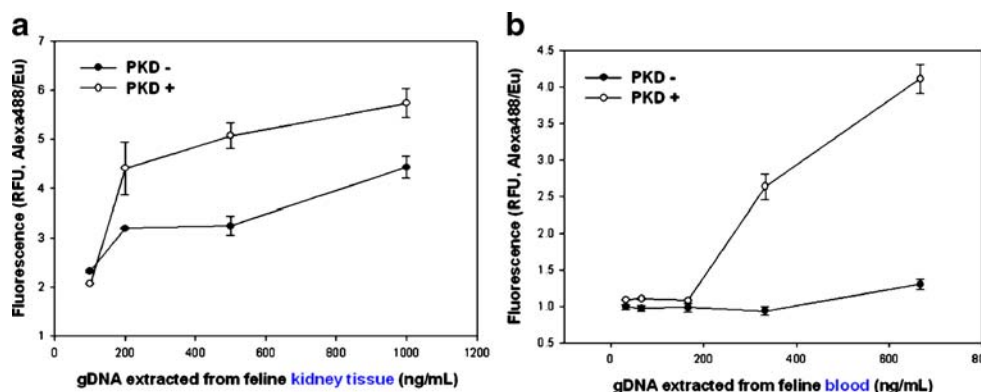
exon38 (Fig. 2b) DNA targets. Following measurement by use of a spectrofluorimeter, the Alexa fluorescence of the target DNAs was normalized with the fluorescence of the NP-probes (i.e. Alexa488/Eu NPs, Alexa647/Tb NPs) for each reaction. This normalization accounts for the fact that intrinsically different numbers of nanoparticles were interrogated in each assay, as a result of variations in the NP numbers that were separated magnetically. PKD (exon29) SNP discrimination was possible over a range of target DNA concentrations (1, 10, 50, 500 pmol L<sup>-1</sup>), while the negative DNA control showed a background fluorescence of 0.2–0.5 RFU (relative fluorescence units) (Fig. 2a). Compared with exon29, the exon38 SNP assay (Fig. 2b) appeared to have less discrimination power in the lower range of DNA target concentrations based on the ratio of fluorescence between PKD positive and negative targets:  $F_{PKD-} / F_{PKD+} = 0.13, 0.35$  for 1, 10 pmol L<sup>-1</sup> target DNA of exon29; versus 0.45, 0.67 for 1, 10 pmol L<sup>-1</sup> target DNA of exon38, respectively. This is likely due to sequence differences of the target SNPs (T-A for PKD+, T-C for PKD- exon29; A-T for PKD+, A-C for PKD- exon38) that resulted in a different strength of Watson–Crick hydrogen bonding between complementary nucleotides of the probe and target DNA. These SNP differences could explain why each complementary pair of DNA probe and target provides a different ability of an assay to discriminate 1 bp mutation. However, statistical values further support that the NPs-DNA-based assay is able to detect SNPs from un-amplified

genomic DNA. In both experiments, the fluorescence of PKD+ and PKD- targets were significantly different based on *P*-values obtained by two-sided *t*-test with 95% confidence level. All corresponding *P*-values were smaller than 0.1: *P*-values =  $8.8 \times 10^{-12}, 6.7 \times 10^{-7}, 1.0 \times 10^{-13}, 1.3 \times 10^{-5}$  (1, 10, 50, 500 pmol L<sup>-1</sup> target DNA of exon29, respectively), *P*-values =  $2.5 \times 10^{-3}, 1.0 \times 10^{-3}, 2.0 \times 10^{-5}, 1.4 \times 10^{-3}$  (1, 10, 100, 1000 pmol L<sup>-1</sup> target DNA of exon38, respectively). Based on the results presented here, this method is feasible for the detection of not only more than one SNP mutation, but also for the quantification of PKD-positive DNA over a dynamic range of target concentrations.

PKD SNPs detection assay for blood and tissue specimens

In the following experiment, genomic DNA (gDNA) was utilized to take advantage of its relative ease of procurement from patient samples, for example from a blood draw or buccal smear or even potentially from cells sloughed into the urine. We first examined gDNA extracted from kidney tissue. Following gDNA extraction from feline kidney tissue, PCR product (~550 bp) targeting the whole region of exon29 of feline gDNA was obtained (Fig. 3) and was subsequently used as a target in the hybridization assay. A PCR product of 550 bp was obtained for both PKD+ and PKD- tissue (Fig. 3). To avoid labeling of target DNA, a signaling DNA probe labeled with Alexa488 was used as a reporter of hybridization. The point mutation in feline PKD

**Fig. 4** PKD SNPs detection in hybridization-in-solution using feline genomic DNA extracted from (a) feline kidney tissue and (b) feline WBC (white blood cells). Successful discrimination of 1 bp nucleotide polymorphism in exon29 gDNA, without PCR amplification, was achieved for both specimens. The signal and error bars represent average and standard deviations based on triplicate reactions



was successfully discriminated in a dynamic range of PCR product concentrations (0.01–10 ng mL<sup>-1</sup>, Fig. 3), when signaling probe was utilized.

Feline blood specimens were examined for PKD SNPs detection in parallel with tissue in subsequent experiments. To further optimize the PKD SNPs assay by avoiding the need of a PCR step, hybridization protocols such as buffer composition and gDNA denaturation conditions were optimized. Variations in the concentrations of formamide and NaCl showed that a combination of 30% of formamide and 75 mmol L<sup>-1</sup> NaCl provides the optimal stringency that allowed SNPs discrimination in genomic DNA (data not shown). Due to the supercoiled and secondary structure of genomic DNA, denaturation by ultrasonication was a critical step in achieving efficient DNA hybridization. While temperature denaturation (95 °C, 5 min) without ultrasonication was not sufficient, the combination of ultrasonication and 95 °C incubation (5 min) transformed gDNA to smaller DNA fragments (data not shown). Fragmented DNA was subsequently used in hybridization reactions as a target. Utilizing a direct hybridization with gDNAs from blood and tissue, detection of PKD SNPs in both samples was successful, as shown in Figs. 4a and b. The detection range of the optimized assay was over 200 ng mL<sup>-1</sup> reaction for both tissue and blood gDNA. We were able to extract a total of 50 µg gDNA from 5 mL whole blood. Since 200–500 ng of gDNA was sufficient to detect SNPs mutations, one could estimate that 0.02–0.05 mL patient whole blood will be a satisfactory sample size. For comparison, we note that a minimum of 0.1 mL feline blood [22] was required for real-time PCR, 300–400 ng of human gDNA [23] for long-range PCR, and 60–120 ng of human gDNA [9, 24] for PCR/sequencing were reported to be used in recent PKD genetic studies. We expect to further improve the sensitivity of the direct hybridization assay by scaling down the reaction volume and performing the assay in a microfluidic device. In those cases where an insufficient amount of gDNA was obtained from clinical specimens, greater sensitivity of the assay could be achieved by amplification of whole gDNA [25–27].

## Conclusions

Magnetic and luminescent nanoparticles can be used for a rapid and quantitative detection of genetic mutations on a hybridization-in-solution platform. By utilizing the advantages of our NPs for SNPs detection in direct hybridization-in-solution, we were able to discriminate genetic mutations of polycystic kidney disease and control gDNA extracted from feline tissue and blood. The proposed non-PCR based PKD SNPs detection method provides a rapid, simple, and inexpensive assay which can easily be translated to a

physician's office or an outpatient clinic using a blood sample, urinalysis, or various other sources of patient genomic DNA. This approach can be extended to SNPs detection in other genetic diseases, and to the detection of cancer-related genes (e.g. the p53 gene), and DNA methylation (studies in progress). The technology has the potential to be engineered into a miniaturized portable device with a micro-channel and simple photo-detector or a high-throughput platform in 96 or 386-well plates for clinical diagnostics. Moreover, the doping of various lanthanide ions into the same host material will be possible in the near future to measure multiple analytes, as we have shown the potential for using two colors of lanthanide oxide (i.e., Eu and Tb) in this study.

**Acknowledgments** We are grateful to Dr Robert A. Grahn and Dr Leslie Lyons in the School of Veterinary Medicine at UC Davis for providing feline kidney tissue and blood. The help of Dr Zhiya Ma in supplying the magnetic iron oxide particles for this study is gratefully acknowledged. This publication was made possible by grant number 5 P42 ES004699 from the National Institute of Environmental Health Sciences (NIEHS), NIH and the contents are solely the responsibility of the authors and do not necessarily represent the official views of the NIEHS, NIH (IMK, KRH). Support was also obtained from the Early Detection Research Network from the NCI (RHW) and grants from the VHL Family Alliance, Dialysis Clinics, Inc., and the Morris Animal Foundation (RHW).

## References

- Gerion D, Chen F, Kannan B, Fu A, Parak WJ, Chen DJ, Majumdar A, Alivisatos AP (2003) *Anal Chem* 75:4766
- Bao YP, Huber M, Wei T, Marla SS, Storhoff JJ, Muller UR (2005) *Nucleic Acids Res* 33:e15
- Zhou X, Zhou J (2004) *Anal Chem* 76:5302
- Qin WJ, Yung LYL (2007) *Nucleic Acids Res* 35:e111
- Storhoff JJ, Elghanian R, Mucic RC, Mirkin CA, Letsinger RL (1998) *J Am Chem Soc* 120:1959
- Storhoff JJ, Marla SS, Bao P, Hagenow S, Mehta H, Lucas A, Garimella V, Patno T, Buckingham W, Cork W, Muller UR (2004) *Biosens Bioelectron* 19:875
- Calvet JP, Grantham JJ (2001) *Semin Nephrol* 21:107
- Dalgaard OZ (1957) *Acta Med Scand* 328:1
- Rossetti S, Strmecki L, Gamble V, Burton S, Sneddon V, Peral B, Roy S, Bakkaloglu A, Komel R, Winearls CG (2001) *Am J Hum Genet* 68:46
- Mochizuki H, Wu G, Hayashi T, Xenophontos SL, Veldhuisen B, Saris JJ, Reynolds DM, Cai Y, Gabow PA, Somlo S (1996) *Science* 272:1339
- Hateboer N, Veldhuisen B, Peter D, Breuning MH, San-Millan JL, Saggarr-Malik AK, Torra R, Dimitrakov D, Martinez I, Sanz de Castro S, Krawczak M, Ravine D (2000) *Kidney Int* 57:1444
- Peral B, Ward CJ, San Millan JL, Thomas S, Stallings RL, Moreno F, Harris PC (1994) *Am J Hum Genet* 54:899
- The European Polycystic Kidney Disease Consortium (1994) *Cell* 77:881
- Son A, Dosev D, Nichkova M, Ma Z, Kennedy IM, Scow KM, Hristova KR (2007) *Anal Biochem* 370:186
- Dosev D, Nichkova M, Dumas RK, Gee SJ, Hammock BD, Liu K, Kennedy IM (2007) *Nanotechnology* 18:055102
- Nichkova M, Dosev D, Gee SJ, Hammock BD, Kennedy IM (2007) *Anal Biochem* 369:34

17. Dosev D, Guo B, Kennedy IM (2006) *J Aerosol Sci* 37:402
18. Lyons LA, Biller DS, Erdman CA, Lipinski MJ, Young AE, Roe BA, Qin B, Grahn RA (2004) *J Am Soc Nephrol* 15:2548
19. Ma ZY, Guan YP, Liu XQ, Liu HZ (2005) *Langmuir* 21:6987
20. Bradford MM (1976) *Anal Biochem* 72:248
21. Dosev D, Guo B, Kennedy IM (2006) *J Aerosol Sci* 37:402
22. Helps CR, Taker S, Barr FJ, Wills SJ, Gruffydd-Jones TJ (2007) *Mol Cell Probes* 21:31
23. Phakdeekitcharoen B, Watnick TJ, Germino GG (2001) *J Am Soc Nephrol* 12:955
24. Veldhuisen B, Saris JJ, de Haij S, Hayashi T, Reynolds DM, Mochizuki T, Elles R, Fossdal R, Bogdanova N, van Dijk MA, Coto E, Ravine D, Norby S, Verellen-Dumoulin C, Breuning MH, Somlo S, Peters DJM (1997) *Am J Hum Genet* 61:547
25. Cheung V, Nelson S (1996) *Proc Natl Acad Sci USA* 93:14676
26. Zhang L, Cui X, Schmitt K, Hubert R, Navidi W, Arnheim N (1992) *Proc Natl Acad Sci USA* 89:5847
27. Dean FB, Hosono S, Fang L, Wu X, Faruqi AF, Bray-Ward P, Sun Z, Zong Q, Du Y, Du J, Driscoll M, Song W, Kingsmore SF, Egholm M, Lasken RS (2002) *Proc Natl Acad Sci USA* 99:5261